Pure & Appl. Chem., Vol.54, No.3, pp.595-610, 1982.
Printed in Great Britain.

0033-4545/82/030595-16$03.00/0
Pergamon Press Ltd

^{13}C NMR OF SOLID POLYMERS AND OF SOLIDS RELATED TO POLYMER COMPOSITES

H. A. Resing, A. N. Garroway, D. C. Weber, John Ferraris*, and
D. Slotfeldt-Ellingsen**

Naval Research Laboratory, Washington, D. C. 20375, U.S.A.

Abstract - Powder anisotropy patterns for the cis and trans isomers of polyacetylene show that δ_3, the principal value associated with the axis perpendicular to the molecular plane, is most affected by the isomeric state (trans - 51 ppm (TMS), cis - 20 ppm, benzene - 1 ppm). Magic angle spinning spectra of bromine doped polyacetylene clearly reveal bromination of the double bond; no Knight shift is observed. In DGEBA epoxy polymers MAS reveals that the phenyl rings of the DGEBA are locked into position at low temperatures in such a way that the phenyl carbons have become inequivalent, as shown by low temperature splittings of their lines. These peaks from inequivalent carbons coalesce pairwise over a broad temperature range to single lines. Our current interpretation is that there is a broad distribution of activation energies for this process, with a mean of 14.3 kcal/mol and a spread of 2.1 kcal/mol. Other more fundamental explanations to this phenomenon are considered. Spectra and derived data are also presented and discussed for (a) partially oxidized poly-thio-tetramethylene, (b) polystyrene-divinylbenzene based ion exchanged resins, (c) surface modified, leached, asbestos fibers, (d) the natural polymers of oil shale, and (e) a model ordered epitaxial system - benzene adsorbed in clay. In connection with the latter, an equation which allows calculation of spectra for partially ordered uniaxial systems is presented; it applies to axially symmetric tensors for any angle between the director and the magnetic field.

INTRODUCTION

High resolution ^{13}C NMR in solids allows the analytical wonders of NMR spectroscopy to be gained for those materials which do not melt or dissolve. In this class of materials we find: a) natural polymers such as oil shale, coal, and wood; b) the electroactive polymer polyacetylene; c) fillers for polymers such as graphite fibers, asbestos fibers, fiber glass, the latter two modified by surface reactions; and d) structural polymers such as the epoxy resins. But over and above analyses, we expect the ordering effect of the solid state to manifest itself, first of all, in an increased number of lines due to the locking in of molecular conformations which might be quite labile in a liquid analogue; and NMR kinetic averaging effects might then become observable. Second, drawing or other forming procedures might order the solid further, resulting in a preferred orientation of a molecule, functional group, or polymer chain segment; kinetic effects appear here as well. For structural polymers, one seeks to understand mechanisms of mechanical loss in terms of molecular motions; the kinetic effects alluded to illumine our path here. In this paper we provide examples of these effects as seen in our laboratory; reference to other work is made as well, but a complete review is not intended. Our principal emphasis here is on the structural, analytic, or kinetic result rather than on the method. Especially pointed out are effects of structural heterogeneity of the specimen on the respective result.

The general field of high resolution NMR in solids has been reviewed recently (Ref. 1); several articles which include ^{13}C NMR of polymers are included there (Ref. 2,3,4,5). The text books of Haeberlen (6) and of Mehring (7) are most useful. Theoretical ruminations regarding ^{13}C experiments in solid polymers are given in Refs. 8 and 9.

Permanent Affiliation:
*University of Texas at Dallas, Dallas, TX, U.S.A.
**Central Institute for Industrial Research, Oslo, Norway.

EXPERIMENTAL ASPECTS

The three major elements (Ref. 10) of the ^{13}C NMR solid state method are a) cross-polarization (proton enhancement), b) proton decoupling, and c) magic angle spinning. By cross polarization is meant the transfer of magnetization from the abundant proton reservoir to the dilute ^{13}C spin system. If this is done under Hartmann-Hahn conditions, the benefits gained are two; the signal strength of the ^{13}C spectrum is enhanced by a factor of four, and the free induction decays (FID's) of the ^{13}C nuclei may be accumulated once every proton T_1 (this latter is a benefit because the proton T_1 is generally substantially shorter than that of the ^{13}C). Proton decoupling is the process of averaging away the dipolar fields, due to the nuclear magnets of protons, that the ^{13}C nuclei normally experience. In principle this could be done by magic angle spinning, but for rigid solids the required rotor speeds of greater than 20 kHz has proven physically prohibitive (Ref. 11). Perhaps the greatest contribution made in the original paper of Pines, Gibby, and Waugh (Ref. 12) was to show that in pulsed ^{13}C NMR one need decouple only during the lifetime of the ^{13}C FID; it is this lowered duty cycle for decoupling which makes the solid state, high-resolution, ^{13}C NMR experiment technically convenient. Magic angle spinning is the process by which chemical shift anisotropies are averaged away to finally yield the ^{13}C high resolution spectrum, and with it the potential for chemical analysis in solids. Once proton decoupling had been achieved (Ref. 12) it was quite obvious from the early work of Andrew (Ref. 13) that such spectra were available. It should be remembered, though, that ^{13}C chemical shift anisotropies are a rich source of structural information, and that magic angle spinning is not de rigueur.

The results listed below were in general obtained under conditions of a) matching the Hartmann-Hahn condition, b) a sufficiently long cross polarization time, TCP, to achieve essentially uniform intensity across the spectrum, c) phase alternation to eliminate pulse feed through and attendant baseline roll, d) single phase detection, e) magic angle spinning speeds of 2-2.4 kHz, f) proton B_1 of 10-12 gauss, and g) a proton frequency of 60 MHz. The repetition period (RP) was in all cases approximately T_1.

The proton channel of our equipment is a Bruker SXP spectrometer. The ^{13}C channel is based on Heathkit amateur radio equipment. In building the probe, the choice of high voltage rf capacitors (especially variable ones) was critical. The magic angle spinner involved the Lowe geometry (Ref. 14) (essentially a barrel rotating on an axle) with boron nitride annular bearings and teflon tubing axles in a teflon yoke; the body was machined of Kel-F, which contains no protons. This simple arrangement does not always yield constant spinning speeds, but nevertheless allows setting and maintaining the magic angle within a degree. Variable temperature was achieved by packing the probe head with glass wool and varying the temperature of the N_2 drive gas: range 150-350 K.

ELECTROACTIVE POLYMERS

The most prized electrical property of synthetic polymers is the dielectric strength. The electrical property most recently commercialized is the piezoelectricity of polyvinylidene fluoride in the form of electro-acoustic transducers. There is great hope that the conductivity induced in conjugated polymers by various dopants (donors, Li, etc. - acceptors, Br_2, AsF_5, etc.) can be fruitfully applied; depending on the level of doping the conductivity of polyacetylene can range from insulator to semiconductor to metallic (Ref. 15). We present here ^{13}C NMR results for the "conductor" polyacetylene and for the "piezoelectric" oxidation products of poly-thio-tetramethylene.

Polyacetylene film, as formed by the Ziegler-Natta polymerization process, consists of a mat of ca. 40 nm diameter fibers, almost randomly interwoven, with a bulk density of about one third that of the true density (Ref. 16). The molecule is a chain of alternating single and double bonded CH units, a conjugated system. There are two isomers as indicated in Fig. 1: cis, formed directly in low temperature (200K) preparations, and trans, which is formed on thermal isomerization (especially above 420 K) of the cis isomer. Now the cis form may have all the double bonds parallel to the chain (cis-transoid), all the double bonds at an angle to the chain (trans-cisoid), or be a mixture of both, with the regions of the two cis forms separated by mobile defects (solitons) (Ref. 17); the degree of mobility of these defects is not known. Magic angle spinning spectra have established mean ^{13}C chemical shifts for the cis (129 ppm) and trans (138 ppm) isomers (Ref. 10, 18, 19). Differences between the two cis forms have not yet revealed themselves, perhaps because the boundary defect is mobile on the NMR time scale at room temperature. Resolution of the magic angle spinning spectra has been sufficiently good to allow quantitative analysis for cis-trans ratio; this ratio does not agree well with results from infra-red spectroscopy on the same specimens (Ref. 19).

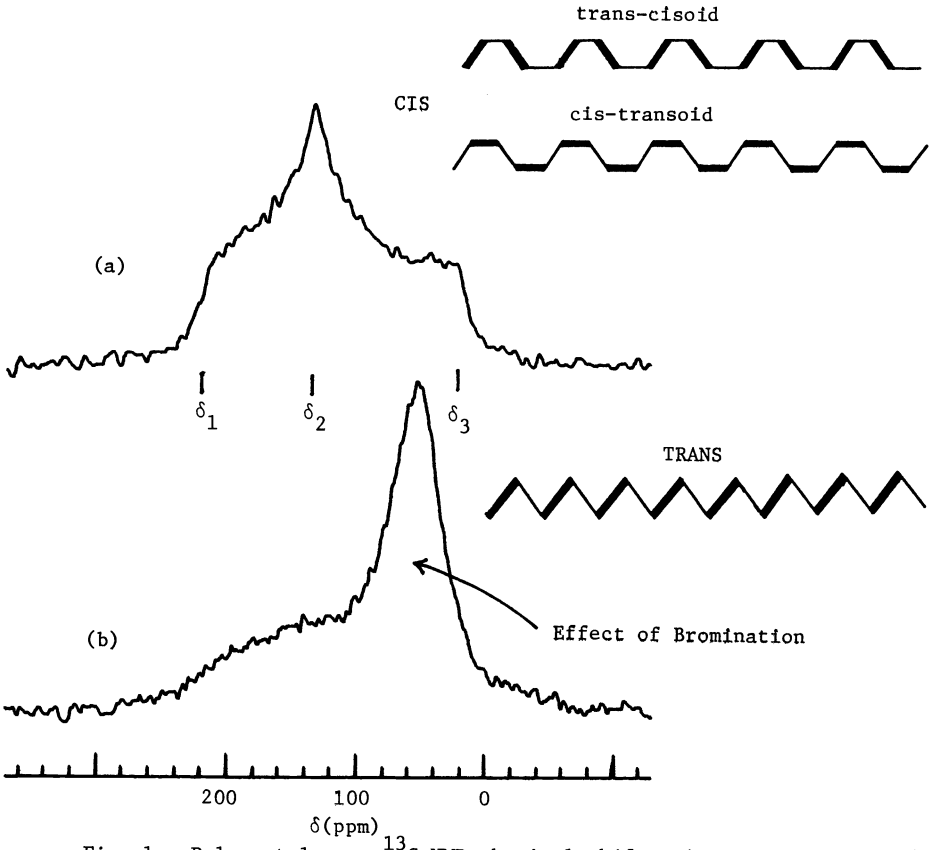

Fig. 1. Polyacetylene. ^{13}C NMR chemical shift anisotropy patterns obtained with proton decoupling and proton enhancement: (a) cis-polyacetylene, 6700 scans, TCP = 800 μs, RP = 5s, T = 77K; (b) brominated trans-polyacetylene ($CHBr_{0.5}$) 200 k-scans, TCP = 800 μs, RP = 1s, T = 300K.

Figure 1a, the powder anisotropy pattern (no magic angle spinning) for a nearly pure cis specimen, shows three singularities, at δ_1, δ_2, and δ_3, each representing a principal value of the chemical shift tensor and a principal axis oriented in the molecular axis system (Ref. 20). By analogy with the benzene molecule it is likely that: principal axis No. 1 (i.e., associated with principal value δ_1, of Fig. 1) lies in the molecular plane, roughly along the C-H bond; principal axis No. 2 lies in the molecular plane perpendicular to axis No. 1; and principal axis No. 3 is perpendicular to the molecular plane (Ref. 21). The value δ_3 appears most sensitive to chemical effects, changing from 20 ppm in the cis isomer to 51 ppm in the trans (Ref. 10). An explanation in terms of the electronic wave functions of the molecule is not yet available. Note that it is this fixed orientation of the principal axis system with respect to a molecular coordinate system which could in principle allow the determination of the molecular axis with respect to the fiber axis; a specimen is required in which the polyacetylene film has been stretched to give a preferred orientation to the fibers, i.e., molecules. Preparation of such a specimen is possible (Ref. 22). And such drawing effects have been seen for polyethylene (Ref. 23). The effect of non-random orientation distributions on the spectrum is well worked out for axial tensors (Ref. 24) as is commented upon below under EPITAXY. For asymmetric tensors, non-random distributions of orientation remain to be treated.

Figure 1b shows the powder anisotropy pattern for a specimen of trans polyacetylene which has been heavily brominated. The peak on the right is ascribed to carbon in brominated double bonds. The underlying broad peak represents the remaining olefinic carbon atoms. Note that the singularities (i.e., sharp corners) of the pure material as seen in Fig. 1a are no longer apparent. A magic angle spinning spectrum for this brominated specimen is shown in Fig. 2b. Here the olefinic carbons are represented by the peak at δ~135 ppm and those in the brominated "double bonds", now sp^3, by the peak at 50 ppm; integration shows that nearly 70% of the double bonds have been lost.

Figure 2a shows the magic angle spinning spectrum of a mostly trans specimen which is somewhat oxidized. The peak at ca. 135 ppm represents trans polyacetylene, the shoulder, cis. The peak at 12 ppm may represent aliphatic content due to crosslinking. In the region 30-100 ppm there is a broad peak, the resolution of which is apparently

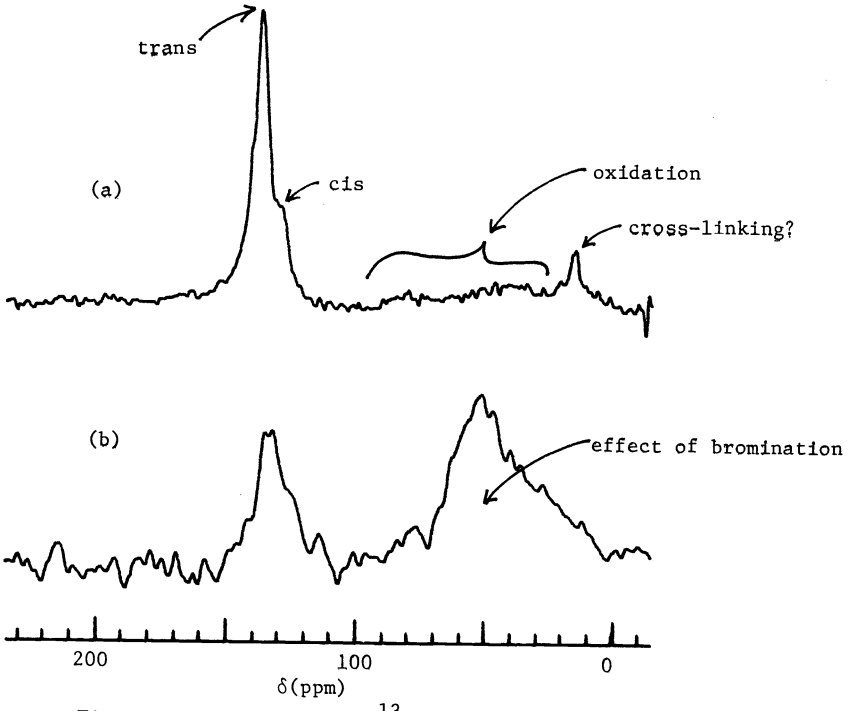

Fig. 2. Polyacetylene. ^{13}C NMR spectra obtained with proton decoupling, proton enhancement, and magic angle spinning: (a) mostly trans-polyacetylene, 24 k-scans, TCP = 800 μs, RP = 0.4s, T = 300K, sample weight = 0.23 g; (b) brominated trans-polyacetylene ($CHBr_{0.5}$), 14 k-scans, TCP = 800 μs, RP = 1s.

not improved by magic angle spinning and the origin of which may be attributed to oxidation products; this region, which accounts for ca. 40% of the signal intensity, shows up much more prominently in the spectrum without spinning (Ref. 10, 25). A spinning spectrum (not shown) for the cis specimen of Fig. 1a shows no oxidation products or cross-linking, i.e., there is a flat baseline away from the cis line.

In Figure 2a the trans and cis lines are not resolved, whereas other investigators have seen such resolution (Ref. 16, 17). In fact, bromination to $CHBr_{0.03}$ of the sample of Fig. 1a serves initially to resolve the trans and cis lines (Ref. 10); the resolution returns to its original value on several hours standing in air (Ref. 10). We believe that ^{13}C linewidths in magic angle spinning spectra of polymers are often caused by distributions of chemical shift due to non-regular packing of molecules (Ref. 3). The "crystal structure" of polyacetylene is ill-defined; nonetheless, best estimates of this structure allow no room for such large dopants as Br_2 (Ref. 26, 27). We speculate that the Br_2 dopant at first gives rise to some dynamic averaging of local environments, due to a "ball-bearing effect", before it is fixed in place due to reaction.

The picture of polyacetylene that emerges from such studies, in agreement with others (Ref. 17) is that despite its molecular simplicity its solid state is quite complicated. Given all the isomers, crosslinks, oxidation products, Br_2 dopants, etc., how do these distribute themselves in space? Is the system homogeneous in any sense? Actually, the line-narrowing due to light bromination, alluded to above, suggests the Br_2 dopant pervades the whole structure and not just the skin of the fibril.

Another insoluble polymer is that formed by oxidizing poly-thio-tetramethylene with H_2O_2 in solution. The product that precipitates is a mixture of unreacted polymer, a sulfone oxidation product, and a sulfoxide oxidation product, as shown with Fig. 3. The intention was that these highly polar groups might lead to a useful piezoelectric material, which has, however, proved not to be the case (Ref. 28). It is not known how these groups are distributed along the chain. Elemental analysis alone cannot decide the sulfone/sulfoxide ratio. Here solid state ^{13}C NMR can help, as the spectrum of Fig. 3 shows. The rather broad line at 32 ppm includes all carbon atoms in the starting material (as shown by the magic angle spinning spectrum of solid poly-thio-tetramethylene) as well as any in methylene groups not α to sulfone or sulfoxide. The line at 52 ppm includes

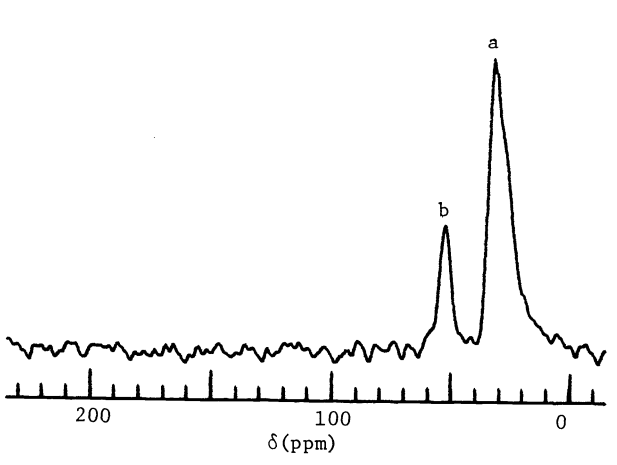

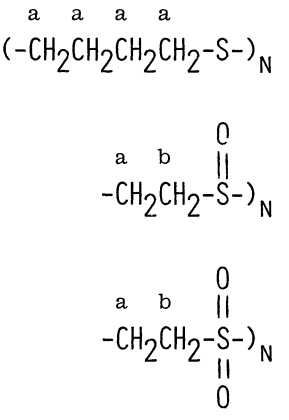

Fig. 3. $(-CH_2CH_2CH_2CH_2S-)_n$, partially oxidized. ^{13}C NMR spectrum, proton enhanced, proton decoupled, with magic angle spinning; 9 k-scans, TCP = 3 ms, RP = 1s, decoupling time = 10 ms, T = 300K.

carbon atoms in methylene groups α with respect to both sulfone and sulfoxide groups (Ref. 29). Because of these degeneracies ^{13}C spectra alone cannot reveal the sulfone/sulfoxide ratio either. However, in combination with elemental analysis there is sufficient information for such a determination. One assumes here that the spectral intensity yields a quantitative measure of the number of carbons in each of the two degenerate lines. Such will only be the case if cross-polarization rates and rotating frame relaxation rates ($T_{1\rho}^{-1}$) are uniform throughout the sample (or if the $T_{1\rho}$'s are long enough so that "equilibrium" cross polarization can be sought for all lines). The status of these rates must be determined by actual measurement, which has not been done for poly-thio-tetramethylene etc. The next section on OIL SHALE takes up this problem.

NATURAL POLYMERS - OIL SHALE

Natural polymers include plant and animal matter in vivo, and derivatives of biomass such as cereal, wood, coal, petroleum and oil shale. By now solid state ^{13}C NMR has been applied to many of these systems (Ref. 33). We have examined a specimen of oil shale to determine the aromatic-aliphatic ratio (Ref. 30). In this system the resolution obtained by magic angle spinning is such that there is a rather broad peak clearly in the aromatic region and another rather broad peak in the aliphatic region. If one takes the spectra as quantitative, this is sufficient to yield the number the petroleum chemists desire - the aromatic-aliphatic ratio, or more simply, the aromatic fraction of carbon atoms.

Now oil shale is a very heterogeneous material, as are most minerals, and there are rigid protocols for sampling in geochemical analysis in order to average such heterogeneity. We chose a monolithic specimen which was ground to the shape of our sample rotor (which of course violates such protocols of sampling). A measurement of $T_{1\rho}$ for the protons showed a nonexponential decay which could be broken roughly into a sum of two exponential decays; this of course indicates some heterogeneity even in this small sample. Are aromatic and aliphatic carbons represented equally in these proton fractions? Our extensive set of experiments (Ref. 30) answers affirmatively and validates ^{13}C NMR as a quantitative analytical tool for this sample. The experiments consisted of varying the cross-polarization time, and recording spectra under otherwise identical conditions at the various TCP. First, the aliphatic intensity followed the proton $T_{1\rho}$ plot very well (Ref. 30), showing that the aliphatic carbons were associated proportionately with the protons of differing $T_{1\rho}$. Second, the aromatic carbon fraction, f_a, was found to be independent of TCP (Fig. 4); this indicates that the solid state ^{13}C NMR experiment gave a quantitative measure of the aromatic fraction, despite the heterogeneity. This method has been used to find a correlation of aliphatic ^{13}C signal strength with oil yield of various shales (Ref. 31). Nevertheless, this short discussion indicates some of the steps which should be taken to validate ^{13}C NMR of solids as a quantitative analytical tool in any given instance.

FILLERS FOR POLYMER COMPOSITES

Composites between structural polymers and fillers often fail at the polymer-filler interface due to weak bonding, perhaps induced by water. One seeks to surface modify

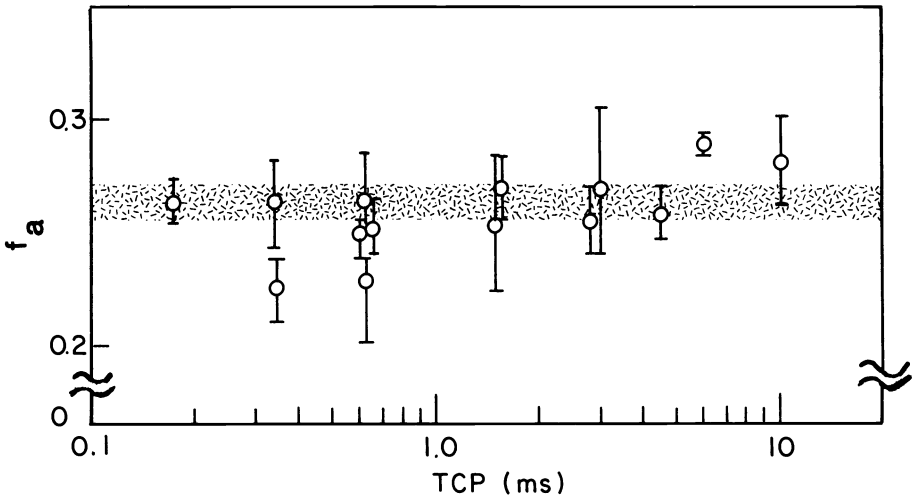

Fig. 4. Oil shale: estimate of aromatic fraction f_a as a function of cross polarization time TCP, as determined from ^{13}C NMR spectra with proton decoupling, proton enhancement, and magic angle spinning. Each point represents a spectrum with 10 k-scans and RP = 0.2s.

such fillers to promote adhesion by covalently bonding to the surface a small molecule with a reactive pendant group. As an example we show in Fig. 5 the spectrum for a leached asbestos - essentially silica gel - which has been reacted with methyl-vinyl-dichlorosilane (Ref. 32) to leave methyl and vinyl groups in one to one ratio; the spectrum of Fig. 5 confirms this very nicely, and we know the reaction went as planned. This was not so with a hoped for allyl derivative, where ^{13}C spectroscopy of solids showed no unsaturation in the product (Ref. 33). Both of these specimens showed about 10% by weight carbon. Thus for this class of solids, which is certainly not soluble, ^{13}C NMR holds promise.

A related applied problem is that in which chromatographic supports are modified by the binding of polymers. Not every commercial chromatographic support has yielded to our ^{13}C analytical efforts however. Despite appreciable carbon contents, $T_{1\rho}$ or proton T_1 difficulties may have conspired against us (Ref. 10). We had great success with chains terminating in phenyl rings. ^{13}C spectra without spinning showed that phenyl rings separated from the silica gel surface by only two or three atoms tended to rotate about the binding point keeping the rings nearly parallel to the surface (Ref. 34). As the chain became longer, more nearly isotropic motions of the phenyl ring became possible (Ref. 34). Other long chain molecules bound to silica gel have recently been studied by magic angle spinning ^{13}C NMR (Ref. 35). One senses here a successful attack on the classical polymer problem of the motions of a polymer molecule bound at one end.

Residual linewidths for ^{13}C magic angle spinning experiments have not passed below 30 Hz in such systems, indicating here as well as in bulk polymers that distributions of shifts arise from "inhomogeneous" molecular packing.

ION EXCHANGE RESINS

Polystyrene-divinylbenzene ion exchange resins represent polymer systems which are also of surface chemical interest. A spectrum for Dowex-1 x 8, chloride form, is shown in Fig. 6, with an assignment of the peaks. This is a medium pore resin containing about 40% water inside the beads. The divinylbenzene cross-linking agent is present at about 8%. Perhaps the most surprising feature is the sharpness of line of the N-methyl carbon atoms. This is remarkable because carbon atoms α to nitrogen in rigid molecules show rather broad doublets, which are expected when the nitrogen atom resides in a site of large quadrupole coupling constant (Ref. 4, 36). Evidently the dipolar field of the nitrogen-14 is well averaged, due to some combination of motions of the quarternary amino-group and ^{14}N self-decoupling due to its own quadrupolar spin-lattice relaxation processes. The N-methyl peak ranges over ~ 1.2 ppm as the counter ion is changed from OH^-, Cl^-, Br^-, to I^-.

We have not yet examined the motions of the phenyl rings by means of analysis of spectra without spinning. Now this specimen consists of a rapidly diffusing phase (the water) and of a non diffusing phase (the resin). Should the pendant phenyl groups show motion in the wet state at room temperature, it would be interesting to see whether freezing the water discontinuously changes the motional state of the phenyl rings.

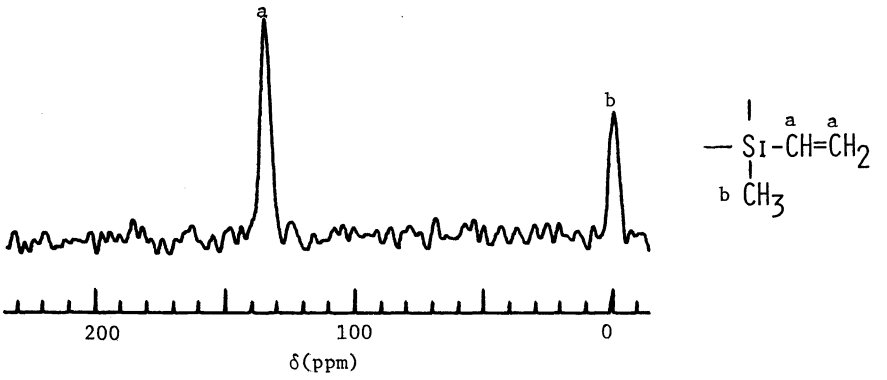

Fig.5. Leached asbestos, modified with vinyl-methyl-dichlorosilane. ^{13}C NMR spectrum, proton enhanced, proton decoupled, with magic angle spinning: 10 k-scans, TCP = 2 ms, RP = 0.3s, decoupling time = 10 ms, sample weight = 0.11 g.

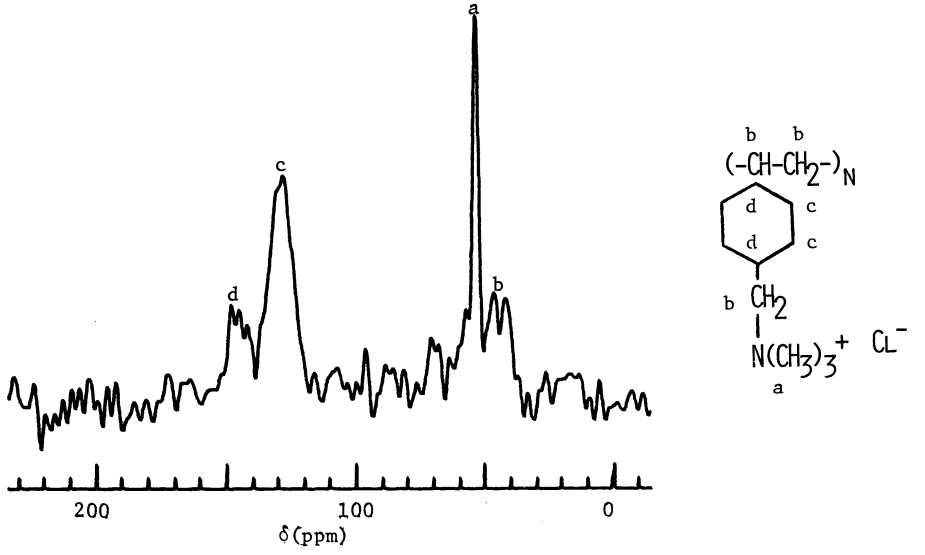

Fig. 6. Ion exchange resin based on polystyrene-divinylbenzene (DOWEX-1); chloride form. ^{13}C NMR spectrum, proton enhanced, proton decoupled, spinning at the magic angle; 10 k-scans, TCP = 6 ms, RP = 0.5s, decouping time = 20 ms, $T_1 \sim 0.3s$, $T_{1\rho} > 60$ ms.

EPITAXY-ORDER

The regular surfaces of clay minerals have been proposed as templates for the organization of polypeptides in the origin of life (Ref. 37). Clays, like graphite, have an interlamellar space in which molecules and ions may be imbibed and spatially ordered (Ref. 38). These organo-clays are not only of interest in themselves, but they serve as models for various ordered states of polymers - drawn, crystalline, and meso-phases. Clay minerals were the original industrial catalysts and catalyst supports; one might search among them for heterogeneous analogues of Ziegler-Natta and other polymerization catalysts; ^{13}C NMR of solids may help.

The specimen we discuss here is ^{13}C enriched (singly labeled) benzene intercalated in an Ag^+ exchanged hectorite clay; the clay was uniaxially ordered by sedimentation from an aqueous dispersion. We desire to know the orientation of the benzene molecule with respect to the clay layers. The tool at hand is the anisotropy of the chemical shift of the carbon-13 atoms of the benzene molecules; the chemical shift depends on the orientation in which the molecule is facing with respect to the magnetic field.

An axially symmetric shift tensor is earier to use for orientation purposes than an asymmetric shift tensor. Even when a molecule like benzene has an asymmetric ^{13}C shift tensor (Ref. 39), as discussed in the polyacetylene section above, rotation about an axis within the molecule (the molecular six fold axis in the case of benzene) converts it to an axial tensor (Ref. 12). The benzene molecule in most of its condensed phases does rotate rapidly about its hexad axis above about 100 K (Ref. 40). The simplicity of the axial tensor can be used for benzene; that is why it was chosen.

The axial tensor has only two principal values: the principal value $\delta_{\parallel}$ is associated with the unique axis (for benzene, the hexad axis), and the degenerate principal value $\delta_{\perp}$ is associated with each of any pair of mutually perpendicular axes which lie in a plane perpendicular to the unique axis. For the benzene molecule, rapid hexad axis rotation erases any information about the C-H bond direction from the remaining chemical shift information; only the orientation of the hexad axis with respect to the magnetic field remains subject to determination.

Recall that the powder anisotropy pattern for ^{13}C in benzene (non-rotating) is almost that of polyacetylene (Fig. 1a) (Ref. 39). Hexad axis rotation serves to average δ_1 and δ_2 so that $\delta_{\perp} = (\delta_1 + \delta_2)/2$; the theoretical <u>random</u> powder pattern then has an infinity at $\delta_{\perp}$. This axial powder pattern is given as

$$P(\delta) = [(\delta-\delta_{\perp})(\delta_{\parallel}-\delta_{\perp})]^{-1/2}/2. \qquad (1)$$

where $P(\delta)$ is the probability of the shift lying between δ and $\delta + d\delta$. If the hexad axes of the molecules have been given some preferred orientation with respect to the magnetic field, this pattern will not be seen, but rather some warping of it. By putting the benzene molecules between the clay layers (which we have aligned by sedimentation) we have put them in a jig or clamp so that we may change their hexad axis orientations collectively as we change the orientation of the normal $\bar{N}$ of the clay film (the director) with respect to a magnetic field $\bar{B}_o$ (with unit vector $\bar{b}_o$ defining its direction). Let γ be the angle between $\bar{N}$ and $\bar{B}_o$ ($\gamma = \cos^{-1}(\bar{N}\cdot\bar{b}_o)$). At every orientation γ we will have a different powder pattern. In Fig. 7a is given the experimental spectrum for $\gamma = 0$, and in Fig. 7c for $\gamma = 90^o$. They are clearly different and not at all like (1), so that we really have a collection of oriented benzene molecules.

Now if all the molecules of a body are held so that congruent axes in each are parallel to the magnetic field $\bar{B}_o$, the resulting spectrum for that orientation of the body will be a delta-function with chemical shift for that orientation. The simplicity of the axial tensor is that for it the converse is true; if a delta-function spectrum is observed, then there is a unique angle β between the unique axis of the tensor (i.e., that of $\delta_{\parallel}$) and $\bar{B}_o$, such that

$$\beta = \cos^{-1}[(\delta-\delta_{\perp})/(\delta_{\parallel}-\delta_{\perp})]^{1/2}. \qquad (2)$$

Fig. 7a is not a delta-function; nevertheless, all the spectral intensity is gathered near $\delta_{\perp}$. This means that when $\bar{B}_o$ is perpendicular to the clay platelets it is also near perpendicular to the hexad axes of the benzene molecules; $\bar{B}_o$ lies in the plane of the molecules. The benzene molecules stand on edge between the clay layers!

Given this orientation of the benzene molecule, it means that the hexad axes of the molecules lie in the plane of the clay film. For $\bar{B}_o$ in the plane of the film, as for Fig. 7c, this means that all orientations of the hexad axis from zero to 2 π with respect to $\bar{B}_o$ are equally likely. The molecule has equal likelihood of presenting ($\delta_{\perp}$) to the field as of presenting its hexad axis ($\delta_{\parallel}$). The result is a two dimensional powder pattern P_{2D},

$$P_{2D}(\delta) = [(\delta_{\perp} - \delta)(\delta - \delta_{\parallel})]^{-1/2}/\pi \qquad (3)$$

much like that of Fig. 7c. The preferred orientation of the benzene molecule is confirmed. Actually this two-dimensional powder pattern will be seen for any uniaxial system in which the director (draw direction) is perpendicular to the magnetic field (Ref. 23).

The ordering of the individual clay layers with respect to the director (i.e., the film normal) is not perfect, nor is the ordering of the molecular hexad axes with respect to the clay layers because of turbostratic arrangements of the layers with respect to each other. To allow for this we define an angle θ between the molecular hexad axis ($\bar{n}$ unit vector) and the film normal ($\bar{N}$ unit vector), so that $\theta = \cos^{-1}(\bar{n}\cdot\bar{N})$, and we let θ be distributed according to some law (Ref. 24). Call the distribution $P_{\theta}(\theta)$. Then for any angle γ of the director $\bar{N}$ with the magnetic field $\bar{B}_o$, where $\gamma = \cos^{-1}(\bar{N}\cdot\bar{b}_o)$, we have a powder pattern (not random!) $P_{\gamma}(\delta)$ given by

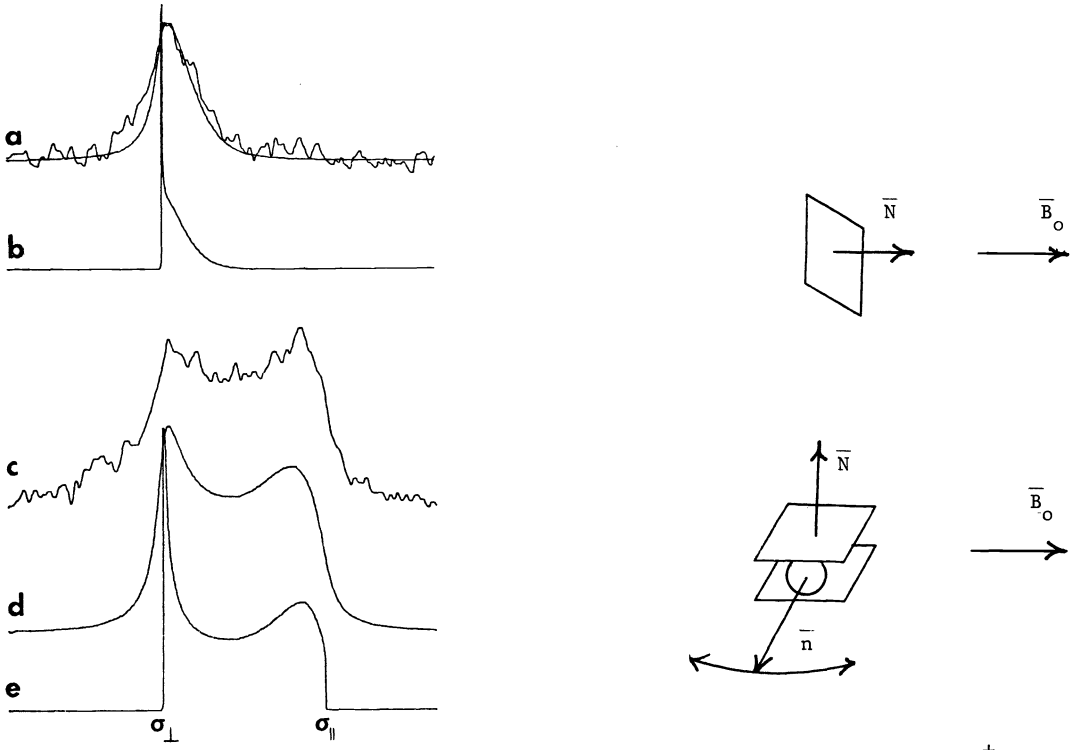

Fig. 7. Benzene intercalated between the layers of an oriented specimen of Ag^+ exchanged hectorite. ^{13}C spectra at 77 K with proton decoupling and proton enhancement. Experiment: (a) magnetic field B_o normal to clay platelets; 10 k-scans, TCP = 2 ms, RP = 0.3s; (c) B_o in the plane of the platelets, 20 k-scans, TCP = 2 ms, RP = 0.3s. Theoretical spectra: b,e) allowing for imperfect alignment of crystallites in the specimen and for imperfect alignment of benzene molecules in the interlayer space; a,d) the same, convolved with a lorentzian line of width derived from higher temperature spectra. See text.

$$P_\gamma(\delta) = [2P(\delta)/\pi] \int_a^b P_\theta(\theta)\, A^{-1/2}\, d\theta \qquad (4)$$

where $A = \sin^2\gamma - \cos^2\theta - \cos^2\alpha + 2\cos\alpha\cos\theta\cos\gamma$

$$\alpha = \cos^{-1}[(\delta - \delta_\perp)/(\delta_\parallel - \delta_\perp)]^{1/2}$$

$$a = \cos^{-1}[\cos(\alpha - \gamma)]$$

$$b = \cos^{-1}[\cos(\alpha + \gamma)].$$

The theoretical spectra in Fig. 7a,b,d,c, represent attempts to fit the experimental data shown, and others, by using a roughly gaussian distribution for $P_\theta(\theta)$ with FWHM of roughly 18 degrees. This will be discussed more fully elsewhere. Special cases of Eq. 4 have been presented earlier (Ref. 24). Normalization of Eq. 4 may be checked by using $P_\theta(\theta) = \sin\theta$, which applies for uniform distribution over a sphere.

In principle, these methods based on the chemical shift tensor apply equally well to dipolar coupling of proton pairs and to deuterium quadrupole coupling interactions. For such cases Eq. 4 represents half the spectrum; its reflection about $\bar{\delta}$ represents the other half (where $\bar{\delta} = (2\,\delta_\perp + \delta_\parallel)/3$).

Motional narrowing of the powder pattern of Fig. 7c has been observed (Ref. 10). It occurs by the process of a central line growing in with loss of intensity of the two-dimensional powder pattern (i.e., the shape of the 2-D powder pattern does not change). This is not the way motional narrowing is expected to proceed for an homogeneous system (Ref. 41). This question is taken up again in the discussion of epoxy ^{13}C NMR spectra below.

EPOXIES, MOLECULAR MOTION

The diglycidyl ether of bis-phenol-A (DGEBA) is the foundation of an industrially most important class of structural polymers. Mechanical properties are most important here. We seek a relationship between features of ^{13}C NMR spectra of cured polymers and their mechanical losses. For DGEBA cured for 16 hours at 393 K with 5% by weight piperidine we now have an extensive set of ^{13}C NMR spectra as functions of temperature (Ref. 42) as well as a very complete study of mechanical loss as a function of temperature (Ref. 43, 44). These are being coupled with new ideas on the physical origin of relaxation processes (Ref. 45) in ongoing work (Ref. 46). Here we analyze the ^{13}C NMR spectral splittings as functions of temperature in terms of a broad distribution of correlation times (Ref. 47); we do this more as a means of bringing to light the issues involved rather than as a means of definitively describing the polymer. Such a description is essayed elsewhere (Ref. 42).

The DGEBA molecule (with one end reacted) is sketched in Fig. 8; ^{13}C magic angle spinning spectra of the cured polymer are given there as well, along with assignment of spectral lines to functional groups. This assignment is based on assignments made in analogous liquid molecules (Ref. 48). Comparison of these spectra with that of solid DGEBA (Ref. 42) and of DGEBA in solution (Ref. 48) show that the line attributable to the unopened epoxide group (the f carbon) is conspicuously absent, as we desire it to be if we are to be concerned with a fully cured resin. The main effects of lowering the temperature are two: line i, due to the methyl carbon, broadens and loses intensity so as to almost disappear at lower temperatures; lines c and d of the phenyl ring become doublets as the temperature is lowered. The loss of methyl group intensity is likely due to an approach of the methyl group rotation frequency to the proton decoupling frequency employed; under these conditions decoupling is not efficient (Ref. 3). The coalesence of doublets, on the other hand, represents some motional narrowing process of the phenyl rings and thus reflects some motion of the polymer backbone; we take the rest of this section to discuss this motional phenomenon.

Why are there doublets at low temperatures? There must be two states of different isotropic chemical shift for both carbons c and d. The proximate chemical cause of this is likely that bond "oxygen-carbon j" is not parallel to the phenyl two-fold axis, nor does it lie in the mirror plane perpendicular to the plane of the ring. In short, the two sites of carbons d are at different distances from carbon j. The same may be said for the two sites of carbons c with respect to the methyl group. For unreacted crystalline monomeric DGEBA, the X-ray structure (Ref. 49) allows crystallographically inequivalent sites for carbons d (and as well for carbons c). In fact, the ^{13}C NMR spectrum of the crystalline solid shows five or six spectroscopically inequivalent sites for carbons d, as discussed elsewhere (Ref. 42). Amorphous DGEBA, on the other hand, shows two lines for carbon d at low temperatures (Ref. 42).

Given a doublet due to nuclear sites of different chemical shift: The collapse of this doublet, as exchange between the sites becomes more rapid, is a staple of NMR lore (Ref. 50). As the exchange frequency τ^{-1} becomes increasingly greater, the lines of the doublet broaden, then merge into a single line, and finally the single line narrows; merger occurs where the product $(\Delta\omega)\ \tau \sim 2$ (where $\Delta\omega$ is the splitting of the original doublet in radians/s). For this simple model of exchange, in no region of exchange frequency is the doublet present along with the narrowed singlet. For doublets which collapse at about room temperature by unimolecular processes the range of temperatures required for the transition from resolved doublet to unmistakable singlet is only about twenty degrees. The data of Fig. 8, as well as additional data not shown, do not support such a model well. First, the temperature range of the transition is almost a hundred degrees (Fig. 8). Second, the coalescence seems to proceed by a filling in of the doublet with a central peak; the narrowed peak at high temperatures appears to be flanked by un-narrowed shoulders. This single correlation time model for collapse of a doublet does not seem to apply, and other models must be considered, as is done below.

This conventional, single-correlation-time picture (Ref. 50) is based on an exponential decay of correlation for the local field as:

$$K_1(t) = \left\langle h(t_o)\ h(t_o + t) \right\rangle_{t_o} \tag{5}$$

$$= h^2 \exp(-t/\tau) \tag{6}$$

where $K_1(t)$ is the correlation function of the time t, h (the local field) is in this case due to chemical shifts and equal to $\Delta\omega/\gamma$, and τ is the mean time between exchange events. Here γ is the nuclear gyromagnetic ratio. The exponential decay of correlation (6), applies to random flights of short duration which occur seldom; for these the poisson distribution of times between flights applies, for which τ is the mean and is called the correlation time.

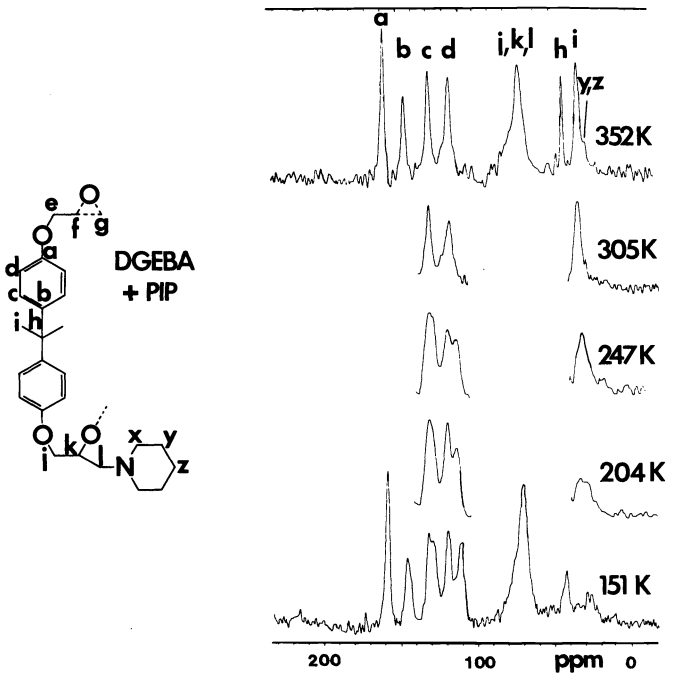

Fig. 8. Epoxy polymer based on DGEBA with 5% piperidine curing agent. ^{13}C NMR spectra at various temperatures, with proton decoupling, magic angle spinning, and proton enhancement; 4000 scans; TCP =1 ms, RP = 1s, decoupling time = 40 ms. The spectra at intermediate temperatures have been simplified to direct attention to the collapse of the doublets in lines c and d and to the narrowing of the methyl peak i.

Quite often this exponential correlation function does not reproduce the experimental result. Dielectric and mechanical relaxations are not Debye-like. NMR relaxation does not follow the picture of Bloembergen, Purcell and Pound. An empirical remedy is the introduction of a distribution of exponential correlation functions. The correlation function then becomes the integral $K_2(t)$:

$$K_2(t) = h^2 \int P(\tau) \exp(-t/\tau) d\tau \qquad (7)$$

where $P(\tau)$, the distribution of correlation times, is chosen either empirically or on the basis of some principle. For example, one might let there be a gaussian distribution in the enthalpy of activation E_a in the Arrhenius law

$$\tau = \tau_o \exp(E_a/RT), \qquad (8)$$

where τ_o, the pre-exponential factor, is an inverse attempt frequency. This distribution in E_a leads to a log-normal distribution for $P(\tau)$ (Ref. 47). Though one may employ a distribution of correlation times it is difficult to be sure whether there are indeed different correlation times (perhaps physically distinct regions of different correlation times) or whether the non-exponential correlation function $K_2(\tau)$ is somehow a true description of the decay of correlation of the local field, a description which pertains to every region of the specimen.

This conundrum may be approached from the opposite point of view. Empirically it has been found that the "Williams-Watts" function, $K_3(t)$, as

$$K_3(t) = h^2 \exp - (t/\tau_p)^{\alpha}, \qquad (9)$$

fits certain dielectric response data quite well (Ref. 51). Ngai (Ref. 45) has recently shown that the form (9) arises quite naturally from a statistical mechanical treatment of relaxation processes, and that it is apparently a correlation function which describes a homogeneous body. Nevertheless, $K_3(t)$ may be worked into the form (7); one can find the corresponding distribution function $P(\tau)$ (Ref. 46). In such a case what does the distribution of correlation times mean? It is nothing more than a way of "parameterizing"

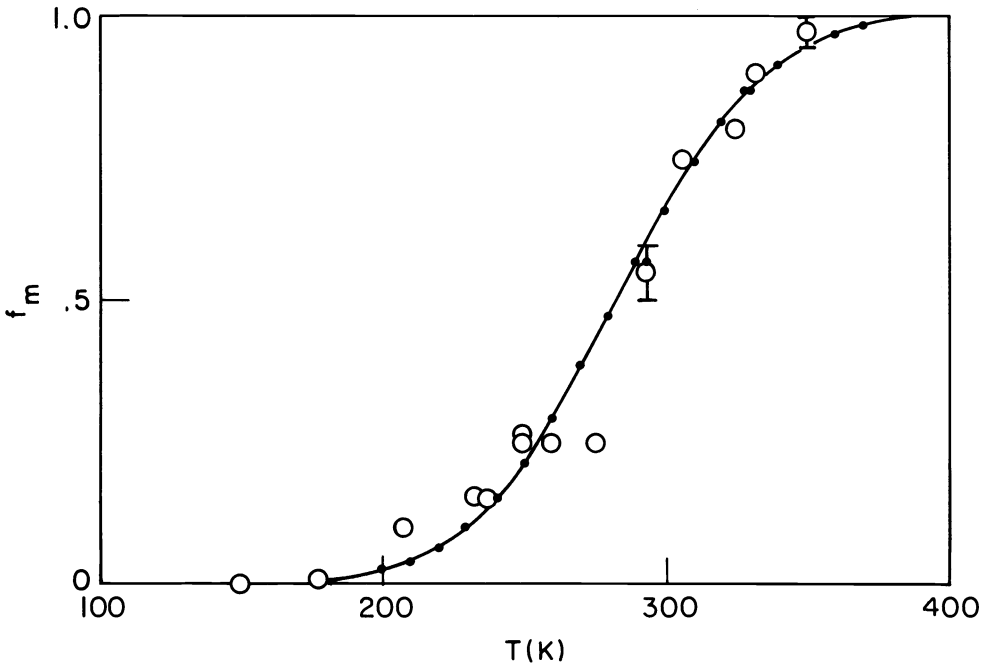

Fig. 9. For the epoxy specimen of Fig. 8: for line d, the fractional intensity of the central singlet as a function of temperature; circles, experimental data, dots, points of theoretical line, i. e., for the distribution of enthalpy of activation as described in text.

the experiment, even though, in a formal sense, one can speak of a distribution of correlation times.

For clarity of presentation, we define two conditions. The homogeneous distribution of correlation times is that parameterization of the true correlation function of the homogeneous body in terms of a formal distribution function for correlation times; it is a purely mathematical representation. The inhomogeneous distribution of correlation times is an attempt to describe molecular motions in a body that is heterogeneous in the sense that the mean time between jumps (the correlation time τ) is a function of position of the jumping entity within the body.

Given this dichotomy between homogeneous and inhomogeneous distributions of correlation times, is there any experimental way of deciding which description is true in a given situation? In the homogeneous case, the NMR spin-lattice relaxation rate T_1^{-1}, using the form (7), is merely the average of the single correlation time relaxation rate over the distribution of τ. In the inhomogeneous case one expects each region to have its own relaxation rate; but averaging may occur by spin diffusion or by molecular diffusion, and the result may then be the same as for the homogeneous case (Ref. 47, 52). For mechanical or dielectric relaxation one observes directly the correlation function and there is no way of deciding its degree of "homogeneity". NMR motional narrowing processes - and the coalescence of the doublet in these epoxies is certainly an example - offer a means of deciding, mainly because the linewidth (in frequency units) can be brought near the molecular motional frequency. Examples of this have been given for motional narrowing of nuclear dipolar broadened lines, for which the inhomogeneous distribution requires coexistence of motionally narrowed and rigid lattice lines at a given temperature (Ref. 47, 53). The progress reported briefly here, and in more detail elsewhere (Ref. 46) is that the collapse of a doublet due to a homogeneous distribution is qualitatively different than that due to an inhomogeneous distribution. Unfortunately the spectral resolution for the data of Fig. 8 is tantalizingly insufficient for an experimental test of this inhomogeneous/homogeneous dichotomy. The effect of a homogeneous distribution on dipolar motional narrowing is not considered here, but was touched on by others at this symposium (Ref. 54, 55).

For a single correlation time the coalescence process has been described. For a homogeneous distribution of correlation times, according to (9), say, the coalescence process resembles that for the single correlation time in that only two peaks are ever resolved; the differences are (a) the region of temperature (i.e., of τ_p) over which coalescence occurs is extended, and (b) the temperature of coalescence is not that at which $\Delta\omega\ \tau_p \sim 2$, but rather a temperature at which $\Delta\omega\ \tau_p \ll 2$ (Ref. 42, 46). For an

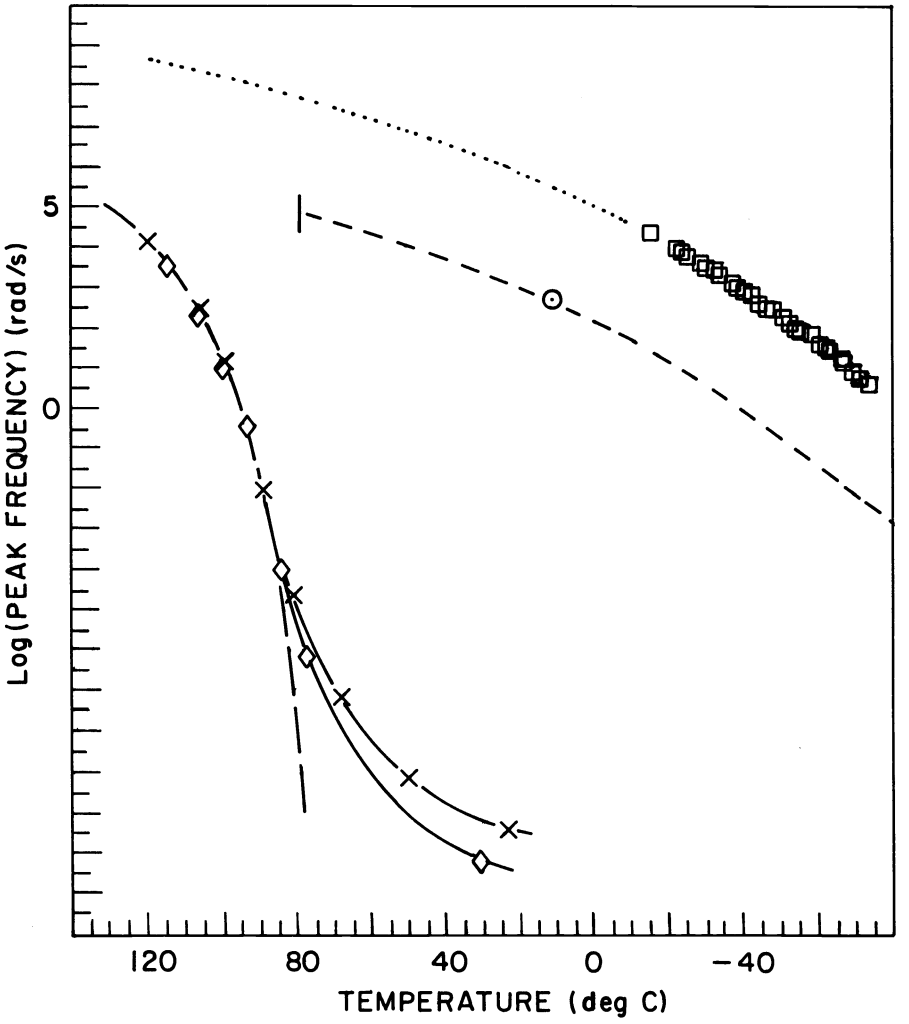

Fig. 10. Comparison of motional frequencies from NMR measurements with those from mechanical loss measurements as functions of temperature for the piperidine cured epoxy. Left side: diamonds and crosses, the α mechanical loss peak. Upper right, squares the β mechanical loss peak. The circle and the dashed line through it: motion of phenyl rings from the ^{13}C NMR spectra. Note that low temperatures are on the right in this figure. The analysis by which the ^{13}C NMR motional frequencies were derived from the data is based on the use of a distribution in the enthalpy of activation; for more complete analysis, see Ref. 42.

inhomogeneous distribution of correlation times (of several decades width), the coalescence process is qualitatively different; as the temperature is raised, the central, coalesced line appears between the lines of the doublet and grows in relative intensity at the expense of the doublet until the doublet disppears. The central line represents those regions for which $\Delta\omega\,\tau << 2$ and the doublet those for which $\Delta\omega\,\tau >> 2$; those for which $\Delta\omega\,\tau \simeq 2$, which are in the coalescence regime in the single correlation time sense, can be taken as a negligible fraction if the distribution is broad enough; but one must keep in mind that one is making this approximation.

Should one expect an inhomogeneous distribution of correlation times to apply for a cured epoxy polymer? The distribution might have its origin in some structural heterogeneity of the polymer body: phenyl groups are present in polymer which reacted first and in that which reacted last; they are at variable distance from points of cross-linking; the body is amorphous, not crystalline. On this basis, phenyl rings in different parts of the body would have spectra in different states of collapse. Let the distribution of barrier heights be gaussian, of standard deviation σ_E; one needs now three parameters to fit the data; τ_o, E_a, and σ_E. The spectrum is to be calculated by adding up the subspectra calculated for each "element" dE of the distribution (Ref. 42, 47). Use the approximation cited above; let the distribution be broad. All the slowly exchanging pairs of sites will be

represented by the doublet, all the fast exchanging ones by the singlet, and that small fraction, close to the critical frequency for exchange, by a collection of partially collapsed spectra which we neglect. We analyze line d of Fig. 8 as sums of singlets and doublets; we use as the experimental parameter the fractional intensity of the singlet, f_m (m for mobile); this is plotted vs temperature in Fig. 9. Theory (Ref. 47) requires this plot to be the cumulative distribution function for the gaussian distribution of activation enthalpies, and it is, as the fitted line shows. Unfortunately, only two of the three parameters τ_o, E_a, and σ_E can be deduced from this plot, and the third must be assumed. Assume $\tau_o = 1.5 \times 10^{-14}$ s; then E_a = 14.3 kcal/mol and σ_E = 2.1 kcal/mol for line d where a doublet splitting of 105 Hz is found. The resulting mean correlation time is to be compared with the mechanical loss data of Ref. 43, 44.

The mechanical loss peak of the same formulation of piperidine cured DGEBA as used in the ^{13}C NMR studies has been determined as a function of temperature by use of a rheogoniometer and time-temperature superposition (Ref. 43, 44). A broad range of peak frequencies has been obtained by liberal use of the time-temperature superposition principle. The results are shown in Fig. 10, where peak frequency is plotted as a function of temperature. Note that temperature increases to the left on this plot. This was done to mimic a plot of reciprocal temperature which NMR spectroscopists normally use, which has low temperature on the right. On such a plot as Fig. 10, the Arrhenius law gives a curved rather than straight line. The α or glass transition peak is on the left; this is of no further interest here. The β peak, expected to be related to chain motion in the cured polymer is at the upper right. The NMR correlation frequency (inverse of the mean correlation time) for the collapse of spectral lines d of Fig. 8 is about 2.5 orders of magnitude below the β-loss peak, but parallel to it. The circle on the NMR τ line represents the temperature at the center of the linewidth transition where $f_m = 1/2$.

The above analysis is based on a broad inhomogeneous distribution of correlation times arising from an assumed gaussian distribution in the enthalpy of activation with FWHM about 30% that of the mean enthalpy of activation. As Fig. 9 shows, it adequately accounts for the spectral shapes as mirrored in the fractional intensity of the central peak. Are we thus to conclude that phenyl ring reorientation and mechanical loss have nothing to do with one another (because they are so far apart in frequency, Fig. 10) and yet have the same activation enthalpy? Perhaps, but the analysis in terms of the homogeneous distribution of correlation times remains to be examined. Further, not all the information available from the mechanical loss study has been used. There time-temperature superposition was assumed to reduce the data; the master curve of Hunston et al (Ref. 43, 44) shows that this assumption fits the data remarkably well. That this is so implies a distribution of correlation times with a temperature independent width and shape. This is at odds with the gaussian distribution in the enthalpy of activation, as used above, which leads to a temperature dependent width. As it turns out, the mechanical loss data for the β relaxation can be described by the Williams-Watts function (9) with $\alpha = 0.28 \pm 0.02$ (Ref. 42); a heterogeneous distribution based on this form fits the f_m data adequately (Ref. 42). Finally, a homogeneous distribution using the form (9) with the mechanical loss α parameter and the theory of Ref. 46 accounts for the line shapes adequately (Ref. 42). Moreover, it brings the jump frequencies for the phenyl ring rotation much closer to the peak frequencies for mechanical loss (Ref. 42); such a unification is one of the goals of this study.

Thus the hoped for test to discriminate between inhomogeneous and homogeneous distributions of correlation times did not quite come about for this epoxy. One must search for systems and stratagems to test these ideas further. For instance, phenyl ring doublets have been produced in polyethylene terephthalate, and there the central peak is clearly resolved in the temperature region of coalescence (Ref. 56). As mentioned above (EPITAXY), for benzene adsorbed in hectorite, the two-dimensional anisotropy pattern also grows a central spike. Heterogeneous distributions do exist, and homogeneous distributions as well. Perhaps proton dipolar or deutron quadrupolar spectroscopies can be brought to bear on the epoxy problem, as has been suggested (Ref. 42).

SUMMARY

Carbon-13 NMR shows itself to be a valuable analytical tool for qualitative and quantitative analysis of polymer functional groups. Spectra for electroactive polymers, polymer fillers, ion exchange resins and epoxies show this. Special ordering effects due to the solid state show up in chemisorbed molecules (polymer fillers) and physisorbed states (benzene on clay) as well as in the epoxy systems. A molecular probing into the dynamic properties of phenyl rings in epoxies is possible. The X-ray structure of the DGEBA monomer must aid in calculating polymer structure and motions. New ways of looking at molecular motions in polymers must be considered.

ACKNOWLEDGEMENT

H. A. Resing thanks Prof. B. Schneider for the invitation to present this lecture in Prague. He thanks Mrs. Mary Jo Tyrrell for preparing the manuscript for publication.

REFERENCES

1. Nuclear Magnetic Resonance Spectroscopy in Solids, The Royal Society, London, 1981; also published as Phil. Trans. Roy. Soc. London, A299, pp. 475-686, 1981.
2. J. Schaefer, E. O. Stejskal, M. D. Sefcik, and R. A. McKay, in Ref. 1, p. 117.
3. A. N. Garroway, D. L. VanderHart and W. L. Earl, ibid, p. 133, see also D. L. VanderHart, William L. Earl, and A. N. Garroway, J. Mag. Res. 44, 361 (1981).
4. G. E. Balimann, C. J. Groombridge, R. K. Harris, K. J. Packer, B. J. Say, and S. F. Tanner, ibid, p. 167.
5. S. J. Opella, J. G. Hexem, M. H. Frey and T. A. Cross, ibid, p. 189.
6. U. Haeberlen, High Resolution NMR in Solids, Selective Averaging, Academic Press, New York, 1976.
7. M. Mehring, High Resolution NMR Spectroscopy in Solids, Springer, Berlin, 1976.
8. A. N. Garroway, W. B. Moniz and H. A. Resing, in Carbon-13 NMR in Polymer Science, ACS Symposium Series, No. 103, Washington, 1979, p. 67.
9. A. N. Garroway, W. B. Moniz and H. A. Resing, Faraday Discussions No. 13, The Chemical Society, London, 1979, p. 63.
10. These elements are discussed briefly, in the same tone as this report, in H. A. Resing, D. Slotfeldt-Ellingsen, A. N. Garroway, D. C. Weber, T. J. Pinnavaia and K. Unger in Magnetic Resonance in Colloid and Interface Science. J. P. Fraissard and H. A. Resing, eds. Reidel, Dordrecht, 1980, p. 239. More complete and authoritative discussions are given in Refs. 1 and 7.
11. E. R. Andrew, Ref. 1, p. 29.
12. A. Pines, M. G. Gibby and J. S. Waugh, J. Chem. Phys. 59, 569 (1973).
13. E. R. Andrew, A. Bradbury, and R. G. Eades, Nature, London 182, 1659 (1958). See Ref. 11 for other references to early work.
14. I. J. Lowe, Phys. Rev. Lett., 2, 285 (1959); see also J. W. Beams, Rev. Sci. Instr. 1, 667 (1930).
15. C. K. Chiang, M. A. Druy, S. C. Gau, A. J. Heeger, E. J. Louis, A. G. MacDiarmid, Y. W. Park, and H. Shirakawa, J. Am. Chem. Soc., 100, 1013 (1978).
16. K. Seeger and W. D. Gill, Colloid & Polymer Sci. 258, 252 (1980).
17. J. C. W. Chien, J. Polym. Sci. Polym. Lett. Ed., 19, 249 (1981).
18. M. M. Maricq, J. S. Waugh, A. G. MacDiarmid, H. Shirakawa, and A. J. Heeger, J. Am. Chem. Soc. 100, 7729 (1978).
19. H. W. Gibson, J. M. Pochan and S. Kaplan, J. Am. Chem. Soc. 103, 4619 (1981).
20. J. F. Nye, Physical Properties of Crystals, Clarendon, Oxford, 1957, for properties of tensors.
21. M. Mehring, op cit, p. 184.
22. C. R. Fincher, Jr., D. L. Peebles, A. J. Heeger, M. A. Druy, Y. Matsamura, A. G. MacDiarmid, Solid St. Comm. 27, 489 (1978); D. L. VanderHart, J. Mag. Res. 24, 467 (1976).
23. S. J. Opella and J. S. Waugh, J. Chem. Phys. 66, 4919 (1977).
24. H. A. Resing and D. Slotfeldt-Ellingsen, J. Mag. Res. 38, 401 (1980).
25. H. A. Resing, in the NRL Program on Electroactive Polymers: First Annual Rept, L. B. Lockhart, ed. NRL Memorandum Rept. 3960, Naval Research Laboratory, Washington, 1979.
26. R. H. Baughman, S. L. Hsu, G. P. Pez, and A. J. Signorelli, J. Chem. Phys. 68, 5405 (1978).
27. H. A. Resing, in the NRL Program on Electroactive Polymers: Second Annual Report. R. B. Fox, ed. NRL Memorandum Rept. 4335, Naval Research Laboratory, Washington, 1980.
28. J. Ferraris, personal communication.
29. Carbon-13 NMR, Sadtler Research Labs. Inc., 1976 Spectra 92C (Butyl sulfone), 1287 C (Butylsulfoxide), and 5134C (Heptyl Sulfide).
30. H. A. Resing, A. N. Garroway, and R. N. Hazlett, Fuel 57, 450 (1978).
31. G. E. Maciel, V. J. Bartuska, F. P. Miknis, Fuel, 58, 155 (1979).
32. L. Zapata, J. Castelein, J. P. Mercier, and J. J. Fripiat, Bull. Soc. Chim. France (1972), 54
33. J. J. Chang, A. Pines, J. J. Fripiat and H. A. Resing, Surf. Sci. 47, 661 (1975).
34. D. Slotfeldt-Ellingsen and H. A. Resing, J. Phys. Chem. 84, 2204 (1980).
35. A. D. H. Clague, personal communication.
36. S. J. Opella, J. G. Hexem, M. H. Frey, and T. A. Cross, Ref. 1, p. 189.
37. N. Lahov, D. White and S. Chang, Science 201, 67 (1977).
38. G. Lagaly, Naturwissenschaften, 68, 62 (1981).
39. M. Linder, A. Hohener, and R. R. Ernst, J. Mag. Res. 35, 379 (1979).
40. E. R. Andrew and R. G. Eades, Proc. Roy. Soc. A, 218, 537 (1953).
41. H. A. Resing, in Magnetic Resonance, etc. as cited in Ref. 10, p. 219; and R. G. Kooser & H. A. Resing, work in progress.

42. A. N. Garroway, W. M. Ritchey, and W. B. Moniz, submitted to Macromolecules. Other papers in this series include Ref. 8 and 9, as well as a) H. A. Resing and W. B. Moniz, Macromolecules 8, 560 (1975) and b) A. N. Garroway, W. B. Moniz and H. A. Resing, Coatings and Plastics Preprints, 36, 133 (1976).
43. D. L. Hunston, W. D. Bascom, E. E. Wells, J. D. Fahey, and J. L. Bitner, in Adhesion and Adsorption of Polymers: Part A, L. H. Lee ed., Plenum, New York 1980, Chapt. 6.
44. D. L. Hunston, W. T. Carter, and J. L. Rushford, in Developments in Adhesives-II, A. Kinloch, ed. Applied Sci. Pub.; London (in press, 1981).
45. K. L. Ngai, Comments on Modern Physics: Part B. IX, 127 (1979); ibid IX, 141 (1979).
46. A. N. Garroway and J. I. Kaplan, in preparation.
47. H. A. Resing, J. Chem. Phys. 43, 669 (1965); H. A. Resing and D. W. Davidson, Can. J. Phys. 54, 295 (1975).
48. S. A. Sojka, W. B. Moniz, J. Appl. Poly. Sci, 1976, 20 (1977); C. F. Poranski, Jr., W. B. Moniz, D. L. Birkle, J. T. Kopfle, S. A. Sojka, Carbon-13 and Proton NMR Spectra for Characterizing Thermosetting Polymer Resins; NRL Report No. 8092, Naval Research Laboratory, Washington, 1977.
49. J. L. Flippen-Anderson and R. Gilardi, Acta. Cryst., in press, 1981.
50. J. I. Kaplan and G. I. Fraenkel, NMR of Chemically Exchanging Systems, Academic Press, New York, 1980, Chapt. 6.
51. G. Williams, D. C. Watts, S. B. Dev and A. M. North, Trans. Farad. Soc. 67, 1323 (1971).
52. H. A. Resing, Adv. Mol. Relax. Processes, 3, 199 (1972).
53. H. A. Resing, ibid, 1, 109 (1968).
54. J. Fahnrich, Poster M32, Prague, 1981.
55. K. Bergmann, Poster M49, Prague, 1981.
56. D. L. VanderHart, personal communication.